Size-Exclusion Effect and Protein Repellency of Concentrated Polymer Brushes Prepared by Surface-Initiated Living Radical Polymerization

Chiaki Yoshikawa,[1] *Atsushi Goto,*[1] *Norio Ishizuka,*[2] *Kazuki Nakanishi,*[3] *Akio Kishida,*[4] *Yoshinobu Tsujii,*[1] *Takeshi Fukuda**[1]

Summary: The adsorption of proteins on poly(2-hydroxyethyl methacrylate) (PHEMA) brushes was systematically investigated from the viewpoint of the size-exclusion effect of the concentrated brushes. By use of surface-initiated atom transfer radical polymerization, well-defined, concentrated PHEMA brushes were successfully grafted on the inner surface of the silica monolithic column with meso pores of ca. 80 nm as well as a silicon wafer and a quartz crystal microbalance (QCM) chip. By eluting low-polydispersity pullulans with different molecular weight through the modified monolithic column, the concentrated PHEMA brush was characterized and demonstrated to sharply exclude solute molecules with the critical molecular size (size-exclusion limit) comparable to the distance between the nearest-neighboring graft points *d*. The elution behaviors of proteins with different sizes were studied with this PHEMA-grafted column: the protein sufficiently larger than the critical size was perfectly excluded from the brush layer and separated only in the size-exclusion mode by the meso pores without affinity interaction with the brush surface. Then, the irreversible adsorption of proteins on PHEMA brushes was investigated using QCM by varying graft densities ($\sigma = 0.007$, 0.06, and 0.7 chains/nm^2) and protein sizes (effective diameter = 2–13 nm). A good correlation between the protein size and the graft density was observed: proteins larger than *d* caused no significant irreversible adsorption on the PHEMA brushes. Thus, we experimentally substantiated the postulated size-exclusion effect of the concentrated brushes and confirmed that this effect plays an important role for suppressing protein adsorption.

Keywords: biocompatibility; biointerface; living radical polymerization; polymer brush; protein; size exclusion

Introduction

Surface-initiated living radical polymerization (LRP) has been explored to yield well-defined polymer brushes with dramatically high graft densities.[1–9] The graft density σ reached as large as 0.7 chains/nm^2 for common polymers like poly(methyl methacrylate) (PMMA) and polystyrene (PS).[9] This density was more than 1 order of magnitude higher than those of typical ''semi-dilute'' brushes, going deep into the ''concentrated brush'' regime which had been little explored systematically because of the unavailability of such brush samples. Our recent studies revealed that these concentrated brushes have structure and properties quite different and even

[1] Institute for Chemical Research, Kyoto University, Uji, Kyoto 611-0011, Japan
E-mail: fukuda@scl.kyoto-u.ac.jp
[2] Emaus Kyoto, Shimotsubayashi, Nishikyo-ku, Kyoto 615-8035, Japan
[3] Graduate School of Science, Kyoto University, Sakyo-ku, Kyoto 606-8502, Japan
[4] Institute of Biomaterials and Bioengineering, Tokyo Medical and Dental University, Chiyoda, Tokyo 101-0062, Japan

unpredictable from those of semi-dilute brushes:[9] most strikingly, the PMMA concentrated brushes swollen in a good solvent (toluene) exhibited an equilibrium film thickness as large as 80–90% of the contour length of the graft chains, indicating that the chains are extended to a similarly high degree.[9,10] Reflecting these characteristic features of graft chain conformation, swollen concentrated brushes brought about unique properties such as extremely strong repulsion against compression and ultra-low friction.[9–13]

As one of the most interesting potential applications of concentrated polymer brushes, attention has been directed toward biointerfaces to tune interactions of solid surfaces with biologically important materials. For example, proteins will adsorb on surfaces through non-specific interactions, often triggering a bio-fouling, e.g., the deposition of biological cells, bacteria, and so on. Attempts have been made to modify surfaces with polymer brushes to prevent protein adsorption. To understand the process of protein adsorption, the interactions between proteins and brush-coated surfaces can be modeled by the three generic modes illustrated in Scheme 1 (after Curie et al.[14] with some modifications). One is the primary adsorption, in which a protein diffuses into the brush and adsorbs on the substrate surface. The secondary adsorption is the one occurring at the outermost surface of the swollen brush film. The last one is the tertiary adsorption, which is caused by the interaction of protein with the polymer segments within the brush layer. For relatively small proteins, the primary and tertiary adsorptions would be particularly important, but they should become less important with increasing protein size and increasing graft density, since a larger protein would be more difficult to diffuse against the concentration gradient formed by the polymer brush, and this gradient, clearly, is a function of graft density. However, the size and density dependence of protein adsorption would manifest itself much more clearly for concentrated brushes due to a different mechanism. As already noted, the graft chains in a concentrated brush are highly extended and hence highly oriented so that the entire brush layer, from the substrate surface to the outermost surface throughout, could have a size-exclusion effect. By the terms ''size exclusion'', we stress the *physical* aspect of the phenomenon, meaning that the protein (or probe molecule) is excluded from the brush layer to avoid the large (mainly conformational) entropy loss caused on the highly extended chains by the entrance of the large molecule, as illustrated in Scheme 2a. Since the degree of chain extension is much less significant in semi-dilute brushes, this effect should be minor for them, and thus even a larger protein will partly diffuse into the brush layer depending on its size (Scheme 2b). Thus concentrated brushes are expected to have a protein repellency effect by this new mechanism of size exclusion and hence much better biocompatibility. This strategy has little been discussed explicitly, although surface-initiated LRP has already been applied for creating novel biointerfaces.

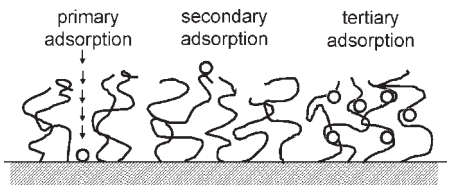

Scheme 1.
Schematic illustration of possible interactions of probe molecules with a polymer brush.

In this work, we will discuss the characteristic size-exclusion effect and excellent protein repellency of concentrated brushes on the basis of our experimental data previously reported with poly(2-hydroxyethyl methacrylate) (PHEMA) brushes.[15,16] PHEMA is a hydrophilic, biocompatible polymer,[17] but the biocompatibility of PHEMA cast film is reported to be not as good as e.g., poly(2-methacryloxyethyl-phosphorylcholine)[18,19] and poly(2-methoxyethylacrylate) cast films.[20,21] Hence any favorable results on the PHEMA brushes could be ascribed more to the structural,

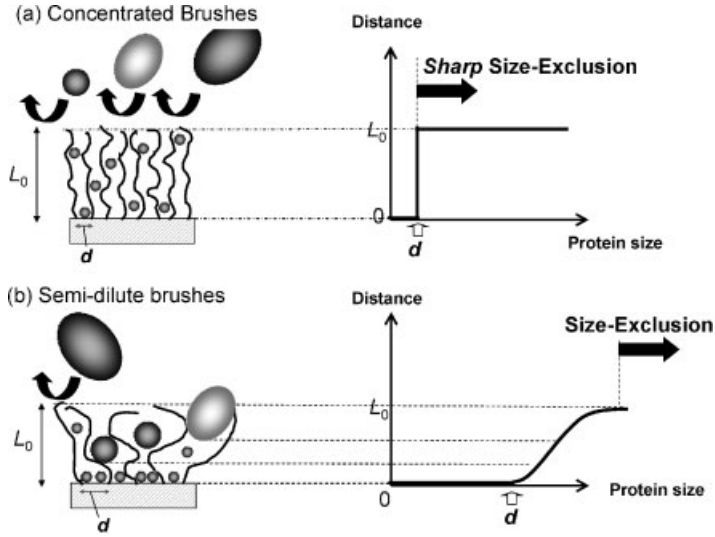

Scheme 2.
Schematic illustration of a size-exclusion effect for (a) concentrated brush and (b) semi-dilute brush. L_0 is the swollen brush thickness and d is the average distance between the nearest-neighbor graft points. The vertical and horizontal axes show the distance from the substrate and the protein size, respectively.

rather than thermodynamic, properties of the system.

Experimental Part

Materials

2-Hydroxyethyl methacrylate (HEMA) (99%, Nacalai Tesque, Japan) was purified according to the literature.[22] An immobilizable ATRP-initiator, 6-(2-bromo-2-isobutyloxy)hexyltriethoxysilane (BHE), was synthesized as previously reported.[23] Bovine serum aprotinin (Aprotinin), bovine serum albumin (BSA), bovine serum immunoglobulin G (IgG), bovine serum thyroglobulin (Thyroglobulin), and horse heart myoglobin (Myoglobin) were purchased from Sigma Co. Ltd. (Osaka, Japan) and used without further purification. All other chemicals were commercially available and used as received.

The monolithic silica material in a rod shape (diameter = 0.5 cm) was prepared and encased according to the literature.[24–26] The pore structure of the monolith was characterized by mercury porosimetry (PORESIZER-9320, Micrometrics, USA). It had meso pores of ca. 80 nm in mean size and surface area of 21 m^2/g.

Silicon wafers were cleaned by ultrasonication in $CHCl_3$ and ultraviolet (UV)/ozone treatment. QCM chips (optically polished square-shaped AT-cut quartz crystals (1×1 cm^2) with gold electrodes) (Seiko EG&G, Seiko Instruments Inc.) were similarly cleaned. On the cleaned chip, Cr and then SiO_2 were deposited in vacuum with the thicknesses of 5 and 40 nm, respectively.

Preparation of PHEMA Brushes

A high-density (concentrated) PHEMA brush was grafted on the inner surface of the silica monolithic column by the immobilization of BHE and subsequent atom transfer radical polymerization (ATRP) of HEMA[27,28] in an on-line (on-column) process using a high-performance liquid chromatography (HPLC) system (see Scheme 3). The BHE-immobilization was conducted by injecting a tetrahydrofuran (THF) solution of BHE (1 wt.-%) and NH_3 (1 wt.-%) at room temperature, and ATRP was conducted by injecting a degassed methanol solution of HEMA (4.5 M),

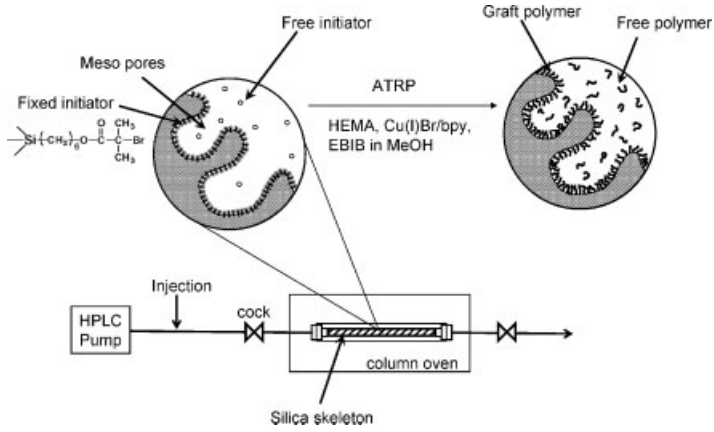

Scheme 3.
Schematic illustration of surface-initiated ATRP by on-line (on-column) process using a HPLC system.

Cu(I)Br (25 mM), bpy (63 mM), and EBIB at 30 °C. The detailed procedure was described elsewhere.[15,16] After the polymerization, the monolithic column was washed by elution of methanol for 24 h to remove free polymers and impurities. The eluted free polymer was analyzed by GPC and used as a good measure in molecular characteristics of the graft polymer. The amount of the grafted PHEMA was determined by elemental analysis.

A high-density (concentrated) PHEMA brush was also prepared on a silicon wafer and a SiO_2-deposited QCM chip by the surface-initiated ATRP.[15] The experimental conditions were the same as those for the on-line (on-column) experiment. The BHE-immobilized substrate was immersed in a degassed polymerization solution, sealed under vacuum in a glass tube, and heated at 30 °C for a prescribed time. After polymerization, the substrate was rinsed in a Soxhlet apparatus with methanol for 5 h to remove physisorbed free polymers and impurities. Lower-density PHEMA brushes were prepared on these substrates by a grafting-to method. Namely, PHEMA chains with an alkoxysilyl group at one chain end were immobilized on a substrate in solution. We prepared two end-functionalized PHEMAs with different chain lengths:[15] the shorter one had $M_n = 1.5 \times 10^4$ and $M_w/M_n = 1.2$, and the longer one had $M_n = 1.2 \times 10^5$ and $M_w/M_n = 1.2$. The immobilization of these polymers yielded a middle- and a low-density brush ($\sigma = 0.06$ and 0.007 chains/nm^2, respectively).

Measurements

The GPC analysis for PHEMA was made on a Tosoh CCP&8020-series high-speed liquid chromatograph (Tokyo, Japan) equipped with two Shodex gel columns LF804 (300 × 80 mm; bead size = 6 μm; pore size = 20-3000 Å) (Tokyo). DMF was used as eluent with a flow rate of 0.8 mL/min (40 °C). The column system was calibrated with Tosoh standard polyethyleneglycols (PEGs). As an absolute number-average molecular weight M_n of PHEMA, the theoretical value $M_{n,theo}$ calculated with the monomer-to-initiator molar ratio and the conversion was used (for selected samples, the validity of this assumption was confirmed by GPC with a multiangle laser light-scattering (MALLS) detector). The following discussion will be based on $M_{n,theo}$ for absolute M_n and $M_{w,PEG}/M_{n,PEG}$ for absolute polydispersity index.

For the GPC analysis of proteins, the above-noted chromatograph equipped with a Shodex gel columns KW804 (300 × 80 mm; bead size = 7 μm; pore size = 300 Å) (Tokyo) was calibrated with

Shodex standard pullulans. PBS was used as eluent with a flow rate of 0.8 mL/min (30 °C).

Chromatograms of pullulans and proteins through the monolithic columns were recorded on a JASCO HPLC system (Jasco co. Ltd., Tokyo, Japan) using PBS as eluent at room temperature. The flow rate was 0.2 ml/min.

QCM analysis was made on a quartz crystal analyzer 917 (Seiko EG&G) driving a 9-MHz QCM chip at 25 °C. The QCM chip was mounted in a thermostated home-made QCM-cell by means of O-ring seals, which allowed only one face of the chip to come in contact with the solution. The Sauerbrey's equation[29] was applied to estimate the adsorbed amount (we confirmed using the QCMs with different fundamental frequencies that the energy dissipation reducing the applicability of this equation was negligibly small in the studied cases).

The dry thicknesses of the PHEMA layers grafted or spin-cast on a silicon wafer or a QCM chip were determined by a spectroscopic ellipsometer (M-2000U^{TM}, J. A. Woolam, NE, USA). The graft density σ was estimated from the dry thickness of graft layer, the M_n value, and the bulk density of PHEMA (1.15 g/cm^3).

Contact angles (θ) were measured at room temperature with a contact angle meter CA-X (Kyowa Interface Science, Saitama, Japan).

Results and Discussions

Size-Exclusion Effect of Concentrated PHEMA Brush

In order to investigate the interaction of the concentrated brush with proteins, we attempted a chromatographic test using a silica monolithic column modified with a well-defined, concentrated PHEMA brush. The chromatographic technique generally provides useful information on the interactions between the analytes and the stationary phase (the brush layer) with a high sensitivity if the stationary phase has a sufficiently large surface area (and volume). The silica monolith with its macro pores of μm size and meso pores of tens of nm size has an extremely large surface area accessible by large molecules like proteins and is ideally suited for our purpose. The on-column surface-initiated ATRP successfully afforded a concentrated PHEMA brush ($M_{n,theo} = 10700$, $M_{w,PEG}/M_{n,PEG} = 1.3$, $\sigma = 0.38$ chains/nm^2) uniformly grafted on the inner surface of the silica monolithic column with ca. 80-nm mesopores.[16] The $M_{n,theo}$ and $M_{w,PEG}/M_{n,PEG}$ values are those for the free polymer with nearly the same molecular characteristics as the graft polymer, and the σ value was estimated from the $M_{n,theo}$ and the amount of grafted PHEMA, which was determined by elemental analysis after all the chromatographic experiments.

A series of low-polydispersity standard pullulans were eluted using PBS as eluent through the PHEMA-grafted monolithic column, and the molecular weight M of pullulans was plotted against elution volume v by the closed squares in Figure 1. The arrowhead on the abscissa in the figure indicates the position of the so-called ''ghost peak'', which is believed to come from low-mass impurities dissolved in the sample solution and correspond to the mobile phase volume v_o. The pullulan-elution curve through the PHEMA-modified column suggests the existence of two modes of size exclusion designated by regions (a) and (b). The region (a) was ascribed to the size exclusion by the meso pores from the similarity with the elution curve for the monolithic column without brushes (data not shown). More interestingly, the v value was sharply shifted in a rather small interval of M in region (b), which was ascribed to the size exclusion by the brush phase for the following reasons. The v value approaches the ghost peak in a low-M region, suggesting that such probe (pullulan) molecules are accessible to the solvent phase even in the brush layer. The horizontal difference corresponding to region (b) is close to the volume of solvent in the brush layer (the

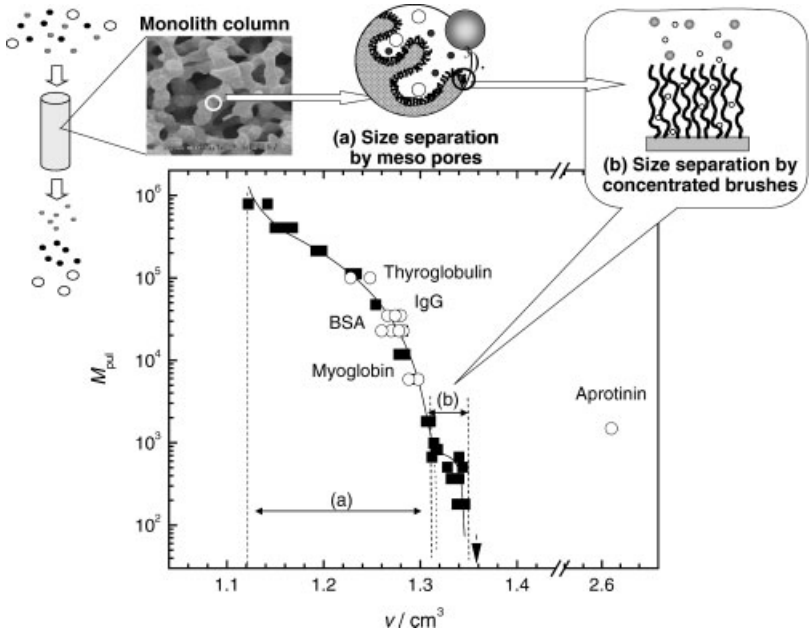

Figure 1.
Plot of molecular weight M_{pul} vs elution volume v for pullulans (filled squares and solid curve) and proteins (open circles) eluted through the PHEMA-grafted monolithic column. The molecular weights of the proteins are the reduced values independently determined by pullulan-calibrated GPC. The arrow head shows the so-called ghost peak of the eluent. The flow rate was 0.2 ml/min with PBS as eluent at room temperature. The inset shows a cartoon illustrating two size-exclusion modes of the brush-modified monolith.

swelling ratio of the PHEMA brush in PBS was estimated to be about 1.5 on a silicon wafer by ellipsometry). This means that almost the whole brush layer is unavailable for the molecules with an M larger than the critical molecular weight about 1000. Here, we calculated the size of pullulan $2R_g$ at $M = 1000$ to be about 1.6 nm, where R_g is the radius of gyration evaluated by using the known relation between the R_g and molecular weight of pullulan.[30,31] It should be noted that this $2R_g$ value is close to the average distance between the nearest-neighbor graft points, $d\,(=\sigma^{-1/2} =$ 1.6 nm). This size exclusion effect must be characteristic of concentrated brushes, in which the graft chains are highly extended and highly oriented so that solutes larger than the distance between the nearest-neighbor graft points d are *sharply* excluded from the entire brush layer, as expected in Scheme 2a.

Interaction of Concentrated PHEMA Brush with Proteins

Then we investigated the elution behavior of proteins with different molecular weights (Thyroglobulin, IgG, BSA, Myoglobin, and Aprotinin) through the PHEMA-grafted column. In order to discuss the interaction of the proteins with the brush, we determined the pullulan-reduced molecular weight M_{pul} of proteins using the conventional GPC columns calibrated with pullulans. Table 1 lists the molecular weight M and the M_{Pul} of proteins as well as the $2R_g$ value evaluated from M_{Pul}. The values of $2R_g$ may be good indices for the protein size (these values of Myoglobin and BSA well agreed with the crystallographically-detemined dimensions).

When these proteins were injected into the BHE-immobilized column (without PHEMA brush), no elution peak was observed. On the other hand, all the proteins injected into the PHEMA-grafted

Table 1.
Absolute and Pullulan-Calibrated Molecular Weights, Crystallographic Dimensions, and $2R_g$ for Studied Proteins.

Protein	Molecular weight M	Pullulan-calibrated M_{Pul}	Crystallographic dimension/nm	$2R_g$[a)]/nm
Aprotinin	6500	1500		2.0
Myoglobin	17000	5900	$3 \times 4 \times 4$[32]	4.5
BSA	67000	22800	$3 \times 8 \times 9$[32–35]	9.9
IgG	146000	35000		12.7
Thyroglobulin	669000	100000		23.4

[a)] Calculated from the known relation between R_g and molecular weight of pullulan.

column were quantitatively recovered as a sharp elution peak. This means that the PHEMA-grafted column caused no such adsorbing interaction with the protein as the BHE-immobilized column did. The M_{pul} value is plotted against the elution volume v for each protein by open circles in Figure 1 (a few elution tests were made for each protein to check reproducibility). The data for the largest four proteins fell on the pullulan-elution curve, suggesting no affinity or adsorbing interaction with the PHEMA-grafted column. More specifically, *those large proteins were perfectly excluded from the brush layer*, separated only in the size-exclusion mode by the meso pores *without affinity interaction with the brush surface*. Reason(s) for this inertness of the brush surface in the interaction with proteins remain to be clarified in terms of static, dynamic, or other properties of solvent-swollen concentrated brushes.

The smallest protein, Aprotinin, was eluted much behind the pullulan of the equivalent size, suggesting a strong affinity interaction with the brush. By analogy of the larger proteins, Aprotinin is also expected to have little affinity interaction with the outermost surface of the brush. Therefore, such interaction may be caused within the brush layer. Here, the question arises as to why Aprotinin can get in the brush, although its molecular weight ($M_{pul} = 1500$) is larger than the above-mentioned size-exclusion limit of the brush layer ($M \approx 1000$). One possible answer to this question may be the difference in shape between Aprotinin and pullulan. Since many proteins are anisotropic (ellipsoidal) in shape, they would get more easily in the brush by an end-on approach, i.e., by setting their long axis normal to the brush surface, than more symmetrical molecules of the same R_g. Another issue to be considered is a local structure of the brush. Generally speaking, even a concentrated brush must have a local distribution in graft density on the substrate surface. Moreover, the effective graft density on the outermost surface of the brush cannot be the same as that on the substrate surface and should be locally fluctuated with time and position. For this reason, even molecules larger than the critical size will also get in the brush layer and stay in there for a certain time.

Irreversible Adsorption of Proteins on PHEMA Brushes with Different Graft Densities

By using QCM, we systematically investigated the irreversible adsorption of proteins on PHEMA brushes by varying graft densities ($\sigma = 0.007$, 0.06, and 0.7 chains/nm^2) and protein sizes (Aprotinin, Myoglobin, BSA, and IgG). The characteristics of the studied surfaces are listed in Table 2. The high-density brush was prepared by surface-initiated ATRP. The middle- and low-density brushes were prepared by the grafting-to method. The hydrophilicities of PHEMA brushes are almost equal to that of the PHEMA cast films independent of their graft densities and thicknesses. This means that the substrate surfaces were perfectly coated with PHEMA. The adsorption of proteins was in-situ monitored by the QCM. For example, BSA was readily (within 10 min) adsorbed, from the PBS solution of BSA (1 g/L), on the low-density brush as well as the BHE

Table 2.
Characteristics of Studied PHEMA Brushes on Substrates.

Surface[a]	$M_{n,theo}$[b]	$M_{n,PEG}$[c]	$M_{w,PEG}/M_{n,PEG}$[c]	L[d]/nm	σ[e]/chain nm^{-2}	d[f]/nm	θ[g]/degree
high-density brush	1.7×10^3	3.5×10^3	1.21	2	0.7	1.2	29
high-density brush	9.7×10^3	8.0×10^3	1.26	10	0.7	1.2	–
high-density brush	16.8×10^3	12.3×10^3	1.30	15	0.7	1.2	29
middle-density brush	19.0×10^3	15.3×10^3	1.27	2	0.06	4.1	27
low-density brush	1.8×10^5[i]	1.2×10^5	1.24	2	0.007	11.9	29

[a] Characteristics of brushes were almost identical on silicon wafers and QCM chips, and typical values on silicon wafers are listed.
[b] Calculated according to $M_{n,theo} = [HEMA]_0/[EBIB]_0 \times MW \times C/100$, where $[HEMA]_0$ and $[EBIB]_0$ are the feed concentration of HEMA and EBIB, respectively, MW is the molecular weight of HEMA, and C is the monomer conversion in %.
[c] Estimated by PEG-calibrated GPC.
[d] Film thickness in the dry state, the error is within 10%.
[e] Graft density calculated with L and $M_{n,theo}$.
[f] Average distance between the nearest-neighbor graft points, calculated according to $d = \sigma^{-1/2}$.
[g] Contact angle, the error is within 2 degrees.
[i] Estimated by GPC with a multiangle laser light-scattering detector.

surface and not desorbed by washing with PBS, indicating an irreversible adsorption. For other proteins, the adsorbed amount, if any, reached almost constant within 1 h. Thus, the amount of adsorbed protein was determined after 1 h of soaking followed by washing with PBS. The PBS washing was expected to remove any weakly/reversibly

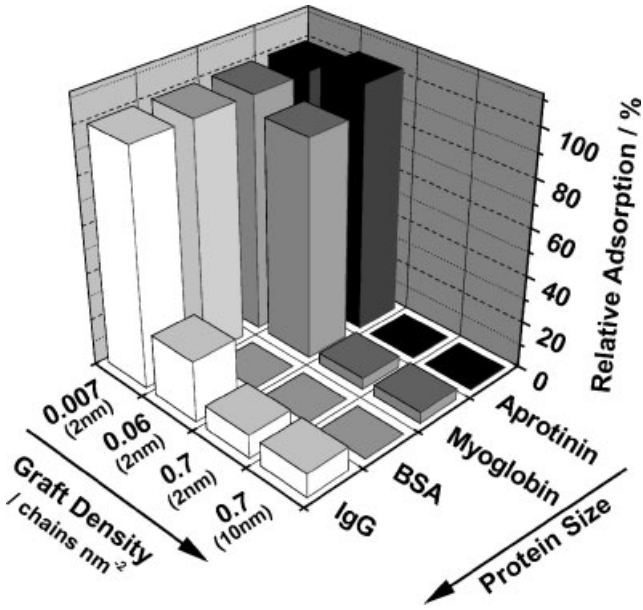

Figure 2.
Irreversible adsorption of proteins onto PHEMA brush surfaces with different graft densities after 1 h of soaking at 25 °C. The protein concentration was 1.0 g/L in all cases. The vertical axis shows the adsorption amount normalized by that adsorbed on the low-density brush ($\sigma = 0.007$ chains/nm^2) for each protein. The values in parentheses along the axis of graft density are the dry thicknesses L.

adsorbed proteins. Figure 2 shows the relative amount of proteins irreversibly adsorbed on PHEMA brushes: the amount of adsorbed proteins was normalized by that adsorbed on the low-density brush for each protein. The low-density brush adsorbed all the proteins, the middle-density one adsorbed only Aprotinin and Myoglobin, and the high-density one, none. These data clearly shows a good correlation between the protein size ($2R_g$: see Table 1) and the graft density, namely, no significant irreversible adsorption of proteins takes place on PHEMA brushes when the brush d was smaller than $2R_g$. All these results confirm that the size-exclusion effect of concentrated brushes plays an important role in the biocompatibility of brush-modified surfaces. We demonstrated by fluorescence microscopy that BSA diffuses deeply into the bulk of the PHEMA-cast film, resulting in an irreversible adsorption mainly by the tertiary adsorption with minor contributions of the primary and secondary ones.

It should be noted that Approtinin caused an affinity interaction with the high-density PHEMA brush (by chromatographic test) but little irreversible adsorption on it (by QCM experiment). This may be due to the difference in graft density: even though these high-density brushes were prepared under the same polymerization conditions, the graft density ($\sigma = 0.38$ chains/nm^2) on the inner surface of the monolith was lower than that ($\sigma = 0.7$ chains/nm^2) on the flat substrate for unclear reason. Aprotinin must be *perfectly* excluded from the brush layer with $\sigma = 0.7$ chains/nm^2 ($d = \sigma^{-1/2} = 1.2$ nm). Another possibility is the fact that the affinity interaction is too weak to cause irreversible adsorption.

We also examined the protein adsorption on the high-density brush with different graft thicknesses $L = 2$ and 10 nm. The high-density brushes with different graft thickness were all free from protein adsorption. This means that a thick brush has a size-exclusion effect from its bottom to the outer surfaces through out. This is the very feature expected for a concentrated brush, as shown in Scheme 2a.

Conclusions

We experimentally verified the idea of protein repellency of concentrated brushes based on their size-exclusion effect: namely when the protein is large enough to perfectly suppress its permeation into the brush layer, no protein adsorption occurs, while when protein is small enough to diffuse into the brush layer, protein adsorption takes place. Furthermore we confirmed the interaction of the concentrated PHEMA brush with proteins is very low at the outermost surface but significant inside. These results strongly indicate that the size exclusion plays an important role in biocompatibility. With other unique properties of concentrated polymer brushes along with a range of possibility to design chain architecture by LRP, PHEMA concentrated brushes will find a wide variety of applications as a novel biointerface, such as biochips, biosensors, bioseparators, and medical body implants.

Acknowledgements: We thank Japan Analytical Industry (Tokyo) for the fractionation of PHEMA by preparative GPC. This work was supported by Grant-in-Aids for Scientific Research, the Ministry of Education, Culture, Sports, Science and Technology, Japan (Grant-in-Aids 17002007 and 17205022).

[1] M. Ejaz, S. Yamamoto, K. Ohno, Y. Tsujii, T. Fukuda, *Macromolecules* **1998**, *31*, 5934.
[2] X. Huang, M. J. Wirth, *Macromolecules* **1999**, *32*, 1694.
[3] K. Matyjaszewski, P. J. Miller, N. Shukla, B. Immaraporn, A. Gelman, B. B. Luokala, T. M. Siclovan, G. Kickelbick, T. Vallant, H. Hoffmann, T. Pakula, *Macromolecules* **1999**, *32*, 8716.
[4] M. Husseman, E. E. Malmstrom, M. McNamara, M. Mate, D. Mecerreyes, D. G. Benoit, J. L. Hedrick, P. Mansky, E. Huang, T. P. Russell, C. J. Hawker, *Macromolecules* **1999**, *32*, 1424.
[5] J.-B. Kim, M. L. Bruening, G. L. Baker, *J. Am. Chem. Soc.* **2000**, *122*, 7616.
[6] B. Zhao, W. J. Brittain, *Prog. Polym. Sci.* **2000**, *25*, 677.
[7] J. Pyun, Y. Kowalewski, K. Matyjaszewski, *Macromol. Rapid. Commun.* **2003**, *24*, 1043.
[8] S. Edmonsdon, V. L. Osborne, W. T. S. Huck, *Chem. Soc. Rev.* **2004**, *33*, 14.
[9] Y. Tsujii, K. Ohno, S. Yamamoto, A. Goto, T. Fukuda, *Adv. Polym. Sci.*, **2006**, *197*, 1.

[10] [10a] S. Yamamoto, M. Ejaz, Y. Tsujii, M. Matsumoto, T. Fukuda, *Macromolecules* **2000**, *33*, 5602. [10b] S. Yamamoto, M. Ejaz, Y. Tsujii, T. Fukuda, *Macromolecules* **2000**, *33*, 5608.
[11] S. Yamamoto, M. Ejaz, Y. Tsujii, T. Fukuda, *Macromolecules* **2002**, *35*, 6077.
[12] K. Urayama, S. Yamamoto, Y. Tsujii, T. Fukuda, D. Neher, *Macromolecules* **2000**, *35*, 9459.
[13] S. Yamamoto, Y. Tsujii, T. Fukuda, N. Torikai, M. Takeda, *KENS Report* **2001–2002**, *14*, 204.
[14] E. P. K. Currie, W. Norde, M. A. Cohen Stuart, *Adv. Collide Interface Sci.* **2003**, *100-102*, 205.
[15] C. Yoshikawa, A. Goto, Y. Tsujii, T. Fukuda, K. Kimura, K. Yamamoto, A. Kishida, *Macromolecules* **2006**, *39*, 2284.
[16] C. Yoshikawa, A. Goto, Y. Tsujii, T. Fukuda, K. Kimura, K. Yamamoto, A. Kishida, *Polym. Prepr., Jpn. (Soc. Polym. Sci., Jpn.)* **2005**, *54*, 5151.
[17] J. P. Montheard, M. Chatzopoulos, D. Chappard, *J. M. S-Rev. Macromol. Chem. Phys.* **1992**, *C32*, 1.
[18] [18a] K. Ishihara, R. Aragaki, T. Ueda, A. Watanabe, N. Nakabayashi, *J. Biomed. Mater. Res.* **1990**, *24*, 1069. [18b] K. Ishihara, N. P. Ziats, B. P. Tierney, N. Nakabayashi, J. M. Anderson, *J.Biomed. Mater. Res.* **1991**, *25*, 1397.
[19] S. Sawada, S. Sakaki, Y. Iwasaki, N. Nakabayashi, K. Ishihara, *J. Biomde. Mater. Res.* **2003**, *3*, 411.
[20] M. Tanaka, T. Motomura, M. Kawada, T. Anzai, Y. Kasori, T. Shiroya, K. Shimura, M. Onishi, A. Mochizuki, *Biomaterials* **2000**, *21*, 1471.
[21] M. Tanaka, A. Mochizuki, T. Motomura, K. Shimura, M. Onishi, Y. Okahata, *Coll. Surf. A Physcicochem. Eng. Aspects* **2001**, *193*, 145.
[22] L. K. Beers, S. Boo, S.G. Gaynor, K. Matyjaszewski, *Macromolecules* **1999**, *32*, 5772.
[23] K. Ohno, T. Morinaga, K. Koh, Y. Tsujii, T. Fukuda, *Macromolecules* **2005**, *38*, 2137.
[24] K. Nakanishi, *J. Porous Materials* **1997**, *4*, 67.
[25] H. Minakuchi, K. Nakanishi, N. Soga, N. Ishizuka, N. Tanaka, *Anal. Chem.* **1996**, *68*, 3498.
[26] N. Ishizuka, H. Minakuchi, K. Nakanishi, K. Hirao, N. Tanaka, *Colloids and Surfaces A: Physicochem. Eng. Aspects* **2001**, *187*, 273.
[27] J.-S. Wang, K. Matyjaszewski, *J. Am. Chem. Soc.* **1995**, *117*, 5614.
[28] M. Kato, M. Kamigaito, M. Sawamoto, T. Higashimura, *Macromolecules* **1995**, *28*, 1721.
[29] G. Z. Sauerbrey, *Phys.* **1959**, *155*, 206.
[30] U. Asolphi, W.-M. Kulicke, *Polymer* **1997**, *38*, 1513.
[31] J. H.-Y. Liy, D. A. Brant, S. Kitamura, K. Kajiwara, M. Mimura, *Macromolecules* **1999**, *32*, 8611.
[32] A. Baszkin, D. J. Lyman, *J. Bio. Mater. Res.* **1980**, *14*, 393.
[33] P. Suttiprasit, V. Krisdhasima, J. Mcguire, *J. Colloid Interface Sci.* **1992**, *154*, 316.
[34] D. C. Carter, X.-M. He, *Science* **1990**, *249*, 302.
[35] F. Hook, M. Rodahl, P. Brzezinski, B. Kasemo, *Langmuir* **1998**, *14*, 729.

